Energy bands and Fermi surface of AuSn

Francis J. Arlinghaus
Research Laboratories, General Motors Corporation, Warren, Michigan 48090
(Received 1 June 1973)

The electronic energy bands and Fermi surface of the ordered intermetallic compound AuSn were calculated using a partially relativistic formulation of the augmented-plane-wave method. A detailed comparison shows the present results to be superior to a nearly-free-electron model. The calculated Fermi surface agrees with experiment, except for one neck orbit.

I. INTRODUCTION

There has been considerable interest in recent years in the Fermi surfaces of metals, particularly as revealed by such low-temperature experiments as the de Haas-van Alphen effect and high-field magnetoresistance. Such studies have been extended to ordered intermetallic compounds since crystals of sufficient purity and stoichiometry have been prepared.

Intermetallic compounds are of considerable interest for the possible light they can shed on the profound problem of alloy phase stability. Extensive experimental data exist on the Fermi surfaces of several β-phase alloys (CuZn, AgZn, PdIn), the fluorite compounds $AuAl_2$, $AuGa_2$, and $AuIn_2$, and more recently, the hexagonal compounds AuSn and PtSn. For all of these but the last, there are theoretical models of the Fermi surface based on exhaustive first-principles energy-band calculations.

The present work extends this theoretical work to AuSn, and presents the author's results on its Fermi surface using the augmented-plane-wave (APW) method for calculating its energy-band structure in a partially relativistic form (but neglecting spin-orbit effects).

AuSn crystallizes in the hexagonal nickel arsenside (NiAs) structure, and is the only known compound of this structure that does not contain any transition-metal atom. The gold atoms reside on a simple hexagonal lattice and the tin on a hexagonal-close-packed lattice. This crystal structure has the space group $P6_3/mmc(D^4_{6h})$ with four atoms per unit cell, the gold at (0, 0, 0) and (0, 0, $\frac{1}{2}$), and the tin at $\pm(\frac{1}{3}, \frac{2}{3}, \frac{1}{4})$. The unit cell is pictured in Fig. 1 and the hexagonal Brillouin zone in Fig. 2. The cell dimensions[1] are $a = 4.3218$ Å, $c = 5.5230$ Å, $c/a = 1.278$.

Various properties of this compound have been studied by Jan *et al.*,[1] one of the most interesting being the striking anisotropy of the thermoelectric power. Jan and Pearson[2] have speculated on the sort of Fermi surface which might explain their results. Sellmyer[3] has studied the high-field magnetoresistance, and finds interesting effects including open orbits. The most revealing study of the AuSn Fermi surface comes from the extensive de Haas-van Alphen measurements of Edwards, Springford, and Saito.[4]

All these workers have attempted to explain their results in terms of a nearly-free-electron model of the band structure. These attempts have met with some success, but fall short of a complete explanation. Furthermore, certain questions do arise. The Fermi-surface topology can be radically affected by splittings of the free-electron bands which arise from the presence of a real crystal potential. The problem arises whether the single-zone or double-zone scheme is more appropriate, because of the degeneracies of the hexagonal top faces of the Brillouin zone. And finally, Jan *et al.*[1] question whether one should postulate the full five electrons per AuSn formula unit available in the normal valencies of the elements, or whether some smaller number would serve better. They cite the fact that AuCs is a semiconductor to show that the question is not trivial.

Because of the large atomic number (79) of gold, it appears that the usual nonrelativistic APW calculation will not be adequate, and that relativistic effects must be included. A fully relativistic treatment in the manner of Loucks[5] is of course possible, but is a very large undertaking, especially in the present case of an alloy with four atoms per unit cell. Fortunately there is a partially relativistic approach available in the manner of Mattheiss,[6] which incorporates the more important effects into a formalism that presents no more computational difficulties than the standard nonrelativistic APW method.

Mattheiss shows that Loucks's expressions for the relativistic APW matrix elements can be rewritten in a form in which two kinds of relativistic effects are clearly separated. The mass-velocity and Darwin corrections, which do not split the nonrelativistic energy levels, are automatically included simply by replacing the usual logarithmetic derivatives of the APW radial functions with

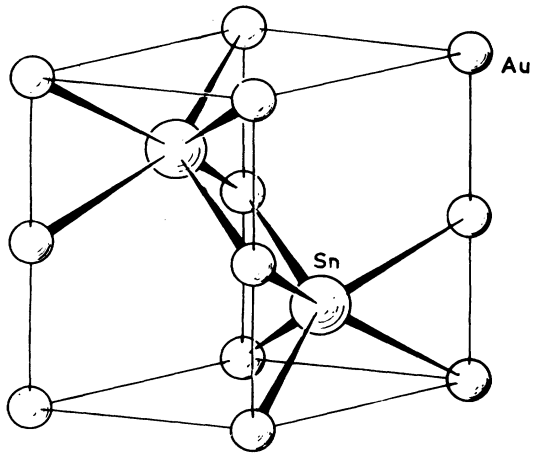

FIG. 1. AuSn unit cell.

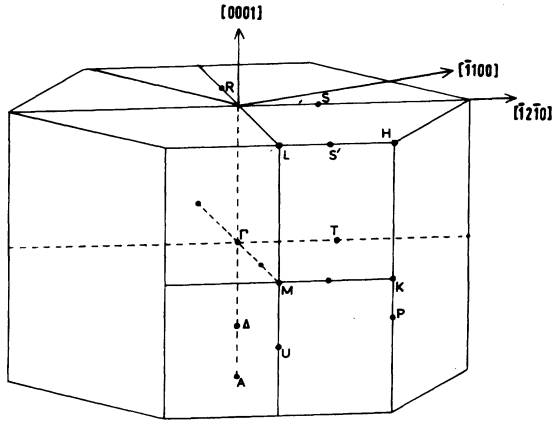

FIG. 2. Hexagonal Brillouin zone.

a relativistic generalization. Spin-orbit corrections, which split energy levels, appear in another term.

If one chooses to neglect spin-orbit splittings (quite a reasonable first approximation in any case), then an approximate or partially relativistic band structure can be obtained by performing what is in all computational aspects an ordinary APW calculation, except that the usual set of logarithmic derivatives are replaced by an "effective" set. These latter are computed in a small auxiliary program, and are done once and for all at the outset (as indeed are the usual nonrelativistic set). If spin-orbit splittings are desired later on, they can be obtained by perturbation theory.

This approach is just what we need here, so we present without further apology the results of a partially relativistic (in the foregoing sense) APW calculation of the energy bands and Fermi surface of AuSn, in which it will be seen that neglect of spin-orbit effects is of little consequence, with one exception that is discussed at length later on.

THE CALCULATION

The usual APW "muffin-tin" potential was generated in a standard manner. Relativistic atomic

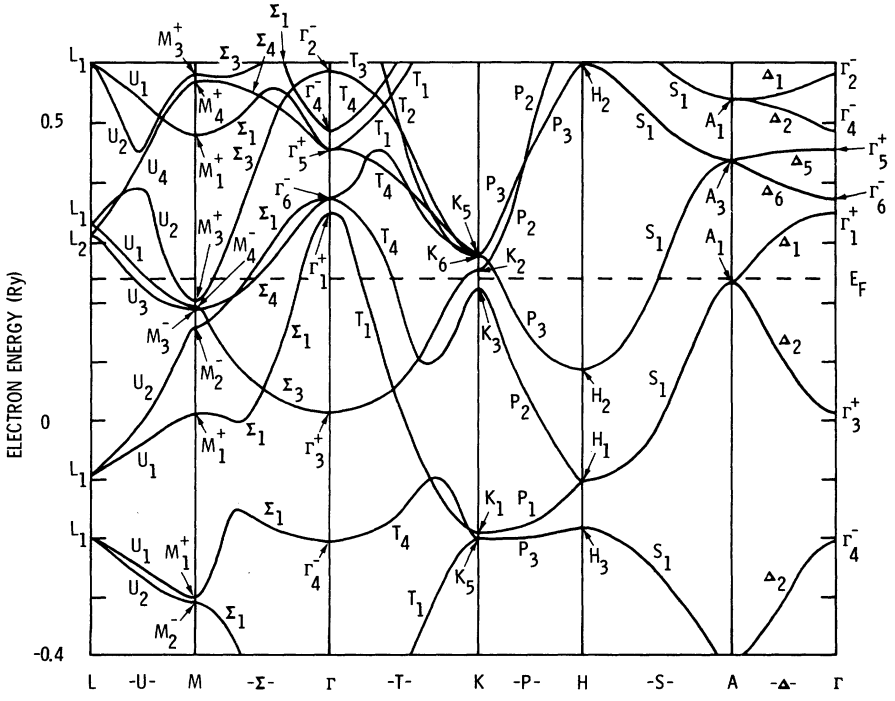

FIG. 3. Energy bands for AuSn.

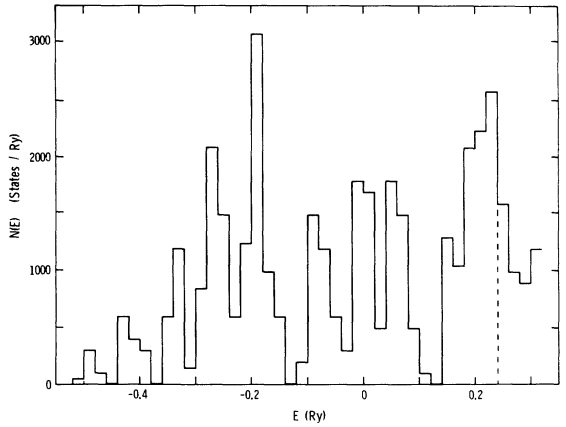

FIG. 4. Density-of-states histogram for AuSn.

charge densities for neutral gold and tin, as determined in a Dirac-Slater atomic calculation,[7] formed the starting point. These assumed a $5d^{10}6s^1$ configuration for gold and a $5s^2 5p^2$ configuration for tin. The spherically averaged contributions of neighboring atoms to this charge density were calculated, the potential was found by integrating Poisson's equation, and this potential was corrected for exchange using the $\rho^{1/3}$ approximation[8] with a coefficient of $\frac{2}{3}$.

The foregoing gives the potential within the APW spheres. Sphere radii were chosen on simple geometrical grounds. The gold radius of 2.609 25 a.u. is just half the gold-gold nearest-neighbor distance, while the tin radius of 2.779 85 a.u. is the difference between the gold radius and the gold-tin nearest-neighbor distance. This straightforwardly gives a well-packed set of nonoverlapping spheres which fills 54% of the space in the crystal.

In the region outside all spheres, the constant average potential is determined from an Ewald problem in the style of Slater and DeCicco.[9] The author has discussed this method previously.[10]

The relativistic equivalents of logarithmic derivatives were generated by solving the Dirac central-field equations using the spherical potentials outlined above. Computer programs for this step were formulated by Koelling[11] and were supplied by him. Energy bands were computed on a regular 144-point mesh in the hexagonal Brillouin zone, using standard APW techniques. The Fermi energy was determined simply by counting states.

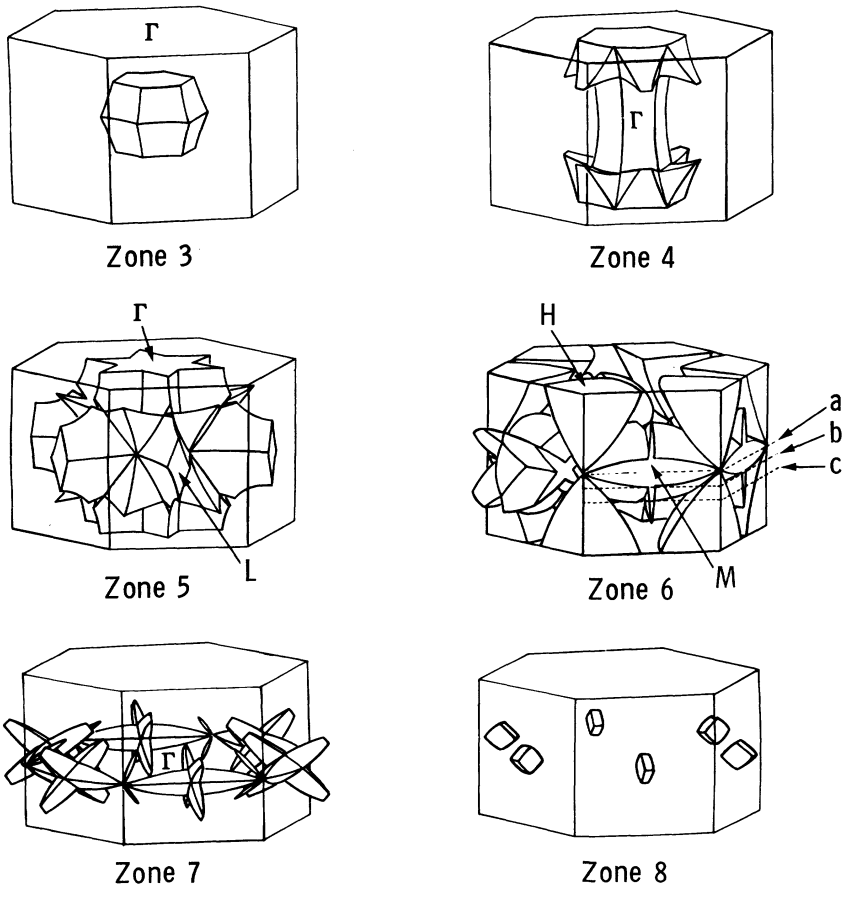

FIG. 5. Free-electron Fermi surface (after Ref. 4).

TABLE I. Theoretical and experimental de Haas-van Alphen frequencies in AuSn.

Orbit	Frequency (10^6 G) 1-OPW[a] model	APW model	Experiment
A_3 ⟨0001⟩	13.0	b	b
A_4 ⟨0001⟩	20.0	b	b
Γ_4 ⟨0001⟩	13.0	14	1.65
Γ_5 ⟨0001⟩	32.8	40	15.4
L_5 ⟨1$\bar{1}$00⟩	3.4	4	1.86
H_5 ⟨0001⟩	73.6	65	69.6
M_5 ⟨11$\bar{2}$0⟩	40	45	59.4
K_6 ⟨0001⟩	b	b	0.71
M_6 ⟨0001⟩	18.3	15	14.9
M_7 ⟨11$\bar{2}$0⟩	16.7	5	4.25

[a] One- orthogonalized-plane-wave model.
[b] Not found.

RESULTS

The computed energy bands of AuSn are shown in Fig. 3 along principal symmetry lines in the hexagonal Brillouin zone. The first point to note is that the gold 5*d* bands do not appear in this figure. They occur at approximately −0.5 Ry on this energy scale—just below the figure—and about 0.75 Ry below the Fermi energy. While the exact position may be somewhat uncertain, the *d*-bands are obviously fully occupied and well below the Fermi energy. This is hardly surprising; indeed it is expected in a nearly-free-electron picture, the electrons from the tin filling a common conduction band to a point well above such *d* bands.

The second point concerns the broad set of conduction bands. Though it may not be obvious at first glance, these bands are, in fact, strikingly similar to free-electron bands for this structure. Essentially all qualitative features of the free-electron bands are reproduced in the calculated APW bands. At the same time, the *quantitative* results are by no means identical. There are large splitting effects at the zone boundaries, and some slight shifts in the relative positions of states. Such things can have profound effects on properties, of course, especially when the states in question are close to the Fermi energy. This will be discussed in more detail in connection with Fermi-surface results.

We show in Fig. 4 a density-of-states histogram for AuSn. While it is quite noisy, there are definitely two large peaks, one about 0.45 Ry below the Fermi energy and the other right at the Fermi energy. The linear temperature coefficient γ in the specific heat is about 4.8 mJ K^{-2} mole^{-1}, or an effective mass of about 1.0 (with perhaps ±20% uncertainty).

The agreement of the predicted Fermi surface with de Haas-van Alphen and magnetoresistance measurements is quite good, but there are considerable differences between the APW and free-electron Fermi surfaces. Figure 5 shows the free-electron Fermi surface, an extremely complicated thing consisting of six sheets. The APW results

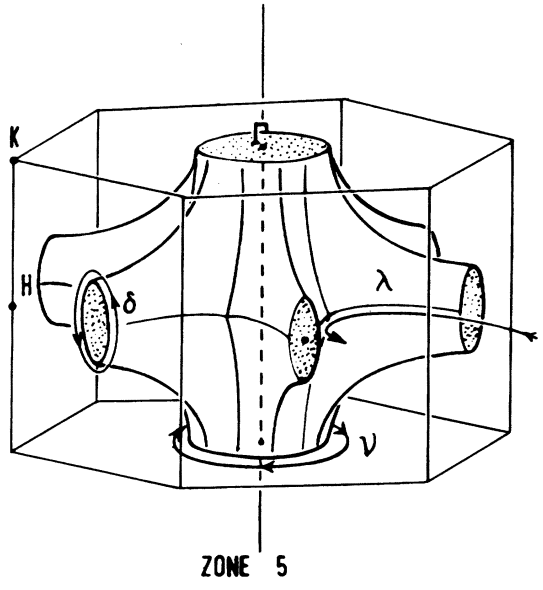

FIG. 6. Fifth-zone sheet of AuSn Fermi surface (after Ref. 4).

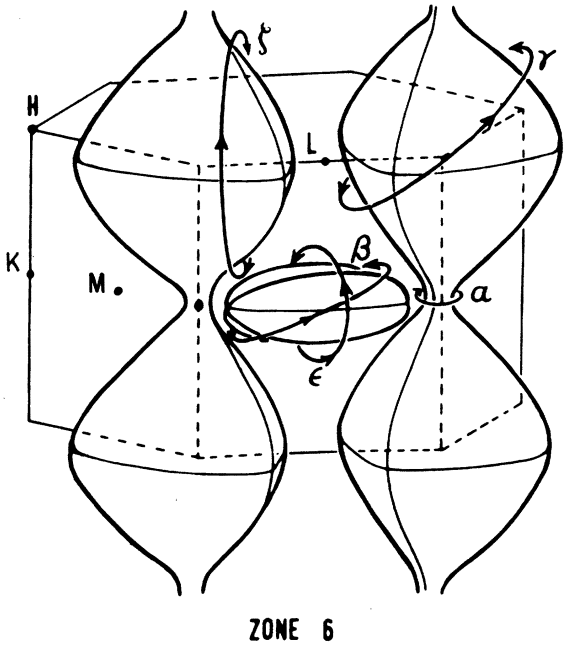

FIG. 7. Sixth-zone sheet of AuSn Fermi surface (after Ref. 4).

have not been found at the high density of points in the Brillouin zone necessary to make really quantitative Fermi-surface models, but they are quite sufficient to indicate the topological features. Some of these are very sensitive to the ordering of certain bands.

A number of de Haas-van Alphen orbit cross sections are listed in Table I, where the present APW predictions are compared with the predictions of a free-electron band model and with the measured values of Edwards *et al.* The APW results agree very well with experiment. We proceed to discuss the various pieces of Fermi surface one by one.

The APW results show that zone 3 is completely filled, unlike the free-electron model, which predicts a sizable hole. This agrees with the results of Edwards *et al.*, who were not able to associate any measured oscillation unambiguously with zone 3. They invoked a double-zone scheme to explain this, but this would appear to be unnecessary. The APW model also finds zone 8 to be empty, again in contrast with the free-electron model, but unlike the zone-3 results, this is not too surprising. It is usual to expect so small a pocket of electrons to disappear in the presence of a potential.

Zone 4 is predicted to have a cylindrical hole, similar to the free-electron result except that the wings are absent and the surface just fails to touch the end faces of the zone. The zone-5 topology is exactly the same as in the free-electron case, but all the sharp corners have disappeared, as in Fig. 6. Zone 7 has pockets of electrons around the M point, but without the complex free-electron "propellers."

All the preceding results are entirely in agreement with the de Haas-van Alphen data of Edwards, Springford, and Saito.[4] Furthermore, the fifth-zone sheet predicts just the kind of open orbits needed to explain Sellmyer's magnetoresistance data.[3]

Zone 6 presents more of a problem. The rounding off of sharp corners typical of real versus free-electron results would tend to produce a surface like that of Fig. 7, which is, in fact, the surface adduced by Edwards *et al.* to explain part of the de Haas-van Alphen data, as well as the anisotropic thermoelectric power measurements of Jan and Pearson.[2] Figure 7 is, in fact, a good picture of the APW-calculated zone-6 surface except for one thing: The pockets at M are found, but the APW band is empty at K, so that the necks completely disappear.

Here we may look back and remember that spin-orbit effects have been left out. The spin-orbit effects are smaller in magnitude than the other relativistic effects (which is part of the justification for neglecting them), but they remove degeneracies and split previously degenerate bands. For nondegenerate states the effect is small because the states cannot be split; but results can be qualitatively different when degeneracies are removed. Since our interest centers on Fermi-surface topology, we will only be concerned with degenerate states at or near the Fermi energy, since splitting such states may change the Fermi surface dramatically.

This can be seen, for example, in the results of Mattheiss on the band structure of rhenium. He shows that there are large energy shifts in going from a nonrelativistic calculation to a partially relativistic calculation of the present type (we, in fact, follow his procedure). But the energy bands with and without spin-orbit coupling are very similar in general location. Those states whose degeneracy is not lifted by spin-orbit coupling (either because there is none to lift or otherwise) appear at almost exactly the same energy with or without spin-orbit coupling.

The dramatic effect of spin-orbit coupling is that it lifts degeneracies. The splitting is usually modest, but the symmetry labels of the states are different and the connectivity of the energy bands can be entirely different. When this occurs to states near the Fermi energy, even slight effects may radically modify the Fermi-surface topology. This is the case with rhenium, because the Fermi energy occurs among the d bands.

In the present case, spin-orbit effects will be few, since little degeneracy exists near the Fermi energy. At M, the states are all nondegenerate, while at A the state A_1 just below the Fermi energy is doubly degenerate, but this degeneracy is not lifted by spin-orbit coupling. The one exception is at K, where there are four states within 0.04 Ry of the Fermi energy, and two of these states, K_5 and K_6, are doubly degenerate. This degeneracy will be lifted by spin-orbit coupling and the states possibly reordered. The magnitude of this effect is difficult to estimate, because the gold and tin contributions will be very different and the percentage character of each in the wave functions for these states is not known. The splitting should, however, be on the order of 0.04 Ry, between the values for gold and tin.[12] It is, however, precisely at this K point that the present results disagree with experiment (and only there). In the absence of a calculation of the spin-orbit splitting at K, the question of the K necks in the Fermi surface must remain in doubt. While it seems possible that this discrepancy between theory and experiment might be explained by the inclusion of the spin-orbit effects, it is not obvious; it depends on the exact numbers involved. At present the expense of a

proper calculation of this effect seems too high a price to pay to explain this one point. It does appear that only this one result will be affected. No other degeneracies appear to lie at sensitive locations.

In conclusion, we note that a partially relativistic APW energy-band calculation for AuSn has successfully produced a model Fermi surface in essential agreement with experiment. One discrepancy remains, which may be due to the neglect of spin-orbit effects, though this is only conjecture. The partially relativistic technique is very convenient for compounds of heavy elements, being no more difficult than a nonrelativistic calculation, but may run into difficulty where the computed property is sensitive to spin-orbit effects.

[1]J.-P. Jan, W. B. Pearson, A. Kjekshus, and S. B. Woods, Can. J. Phys. 41, 2252 (1963).
[2]J.-P. Jan and W. B. Pearson, Philos. Mag. 8, 911 (1963).
[3]D. J. Sellmyer, J. Phys. Chem. Solids 30, 2371 (1969).
[4]G. J. Edwards, M. Springford, and Y. Saito, J. Phys. Chem. Solids 30, 2527 (1969).
[5]T. L. Loucks, Phys. Rev. 139, A1333 (1965).
[6]L. F. Mattheiss, Phys. Rev. 151, 450 (1966).
[7]D. Liberman, J. T. Waber, and D. T. Cromer, Phys. Rev. 137, A27 (1965).
[8]J. C. Slater, Phys. Rev. 81, 385 (1951).
[9]J. C. Slater and P. D. DeCicco, MIT Solid-State and Molecular Theory Group Quarterly Progress Report No. 50, 1963 (unpublished), p. 46.
[10]F. J. Arlinghaus, Phys. Rev. 186, 609 (1969).
[11]D. D. Koelling (private communication).
[12]F. Herman and S. Skillman, *Atomic Structure Calculations* (Prentice-Hall, Englewood Cliffs, N. J., 1963).